Discover Oncology

Analysis

Development and validation of a multiple myeloma diagnostic model based on systemic lupus erythematosus-associated genes and identification of specific genes

Yuepei Liu[1] · **Songshan Liu**[2]

Received: 19 November 2024 / Accepted: 2 May 2025
Published online: 18 May 2025

Abstract

Background Monoclonal immunoglobulins are commonly found in multiple myeloma (MM), a prevalent hematologic malignancy that is currently incurable. In recent years, the association between systemic lupus erythematosus (SLE), an autoimmune disease, and MM has garnered increasing attention. However, there remains a lack of in-depth research regarding the interactions between these two conditions and their potential pathogenic mechanisms. Therefore, in order to improve the identification of MM associated with SLE, this work attempts to clarify the pathogenic pathways that are shared by MM and SLE and to develop corresponding diagnostic models.

Methods This study employs a comprehensive bioinformatics analysis combined with machine learning techniques to extract relevant data from public databases. We used GO and KEGG pathway analyses to investigate the functionalities and pathway enrichments of the DEGs that we found in MM and SLE populations. Furthermore, we used the STRING database to build a PPI network for the intersecting genes and the cytoHubba plugin in Cytoscape software to identify important genes with biological significance. To establish a diagnostic model for SLE-related MM, we compared 113 combinations of 12 machine learning algorithms, ultimately determining the optimal model.

Results Our analysis identified 63 intersecting genes, with 31 exhibiting upregulated expression and 32 showing downregulated expression. The selection of key genes indicated that nine genes met the criteria of having both Degree and MCC values exceeding 3, among which seven (CDH1, IL4, AURKB, HGF, H2BC9, AREG, TJP1) have previously been confirmed to have direct associations with MM. Notably, H2BC5 was identified as a specific gene associated with SLE-related MM. Our findings revealed that elevated expression of H2BC5 is significantly correlated with an increased risk of MM, suggesting its potential critical role in the diagnosis and identification of this malignancy.

Conclusion A new molecular framework for the early diagnosis of MM, especially in SLE patients, is established by this study. Our findings highlight H2BC5 as a possible biomarker that merits more research into how it contributes to the development of MM. By identifying the shared pathogenic mechanisms between SLE and MM, our research offers new perspectives for future clinical interventions and personalized therapies.

Keywords Multiple myeloma · Systemic lupus erythematosus · Machine learning algorithms · Mendelian randomization · Bioinformatics

Supplementary Information The online version contains supplementary material available at https://doi.org/10.1007/s12672-025-02555-7.

✉ Songshan Liu, 18628190985@163.com | [1]Chengdu University of Traditional Chinese Medicine, Chengdu 610075, China. [2]Department of Hematology, Affiliated Hospital of Chengdu University of Traditional Chinese Medicine, Chengdu 610075, China.

1 Overview

Multiple myeloma (MM), a malignant tumor of plasma cells that originates in the bone marrow, is characterized by a notable clonal proliferation of abnormal plasma cells. During the course of the disease, osteolytic lesions cause hypercalcemia, spinal cord compression, and excruciating bone pain in up to 90% of myeloma patients [1–3]. MM is the second most frequent hematologic malignancy worldwide, behind non-Hodgkin lymphoma, and makes up 1.3% of all malignant neoplasms and 14% of hematologic malignancies [4, 5]. Even though MM treatment has advanced significantly in the last ten years, most patients still die from the high rates of medication resistance and recurrence linked to traditional chemotherapy. Patients with high-risk MM continue to have a five-year survival rate of 50% or less [6, 7].

Dysregulation of immune responses and the development of autoantibodies are hallmarks of systemic lupus erythematosus (SLE), a moderately common chronic systemic autoimmune rheumatic illness that often affects several organ systems [8]. A growing amount of evidence suggests that SLE is linked to a higher risk of developing many types of cancer and is a leading cause of death from a number of cancers, particularly hematopoietic system tumors. With a standardized incidence ratio (SIR) of 8.9 (95% CI, 3.90–12.48), the risk of MM is very high [9–11]. Studies have found that the majority of patients develop MM several years after being diagnosed with SLE [12, 13]. Therefore, early identification of potential MM in patients with SLE is particularly important. However, MM and SLE patients frequently describe non-specific symptoms during their initial appointments [14, 15], this could result in situations being overlooked or misdiagnosed. In order to help in the early detection of possible MM in patients with SLE, a thorough diagnostic model must be developed immediately.

Initiating medical intervention requires early disease identification. Finding the right biomarkers is essential to solving this pressing problem. Finding possible biomarkers is made easier by the development of machine learning and bioinformatics technology [16, 17]. Mendelian randomization (MR), a potent epidemiological research technique, usually uses genetic variants as instrumental variables (IV) to ascertain the causal links between risk factors and diseases [18].

By looking at and evaluating two SLE microarray datasets and three MM microarray datasets from the Gene Expression Omnibus (GEO) collection, this work uncovers possible processes connecting SLE and MM. Additionally, we created a diagnostic model for SLE-related MM using a computational framework that contains 113 combinations of 12 machine learning techniques. The study also analyzes immune cell infiltration in SLE and MM. Furthermore, we investigate the correlations and causal linkages of important genes in the pathogenesis of SLE-related MM by expression quantitative trait loci (eQTL) and MR studies. To our knowledge, no previous investigations have revealed the putative functional pathways and pathogenic processes between SLE and MM. In this research, we intend to employ sophisticated bioinformatics and machine learning approaches to uncover important biomarkers strongly associated with SLE-related MM, thereby boosting clinical detection, diagnosis, and prevention of possible MM in patients with SLE.

2 Materials and methods

2.1 Source of raw data and data preprocessing

Using the keywords"multiple myeloma"and"systemic lupus erythematosus,"we followed the selection criteria from previous literature to identify four transcriptomic datasets (GSE5900, GSE6477, GSE61635, GSE50772) from the NCBI GEO (https://www.ncbi.nlm.nih.gov/geo/) database as the training set, while GSE118985 was reserved for validation. The GSE24080 and GSE57317 datasets were utilized for survival analysis. The batch effects between the datasets were corrected and the data were merged using the"SVA"package in R. Principal component analysis (PCA) was performed using the Prcomp function from the stats package in R [19]. Additionally, the ggplot2 package was employed to visualize the data, enabling a comparison of data quality before and after batch effect removal. Detailed information about these datasets is provided in Table 1, including platform specifics and sample grouping information.

This study collected summary data for eQTL from the GWAS Catalog website as exposure data, while outcome data were sourced from the latest version R11 of the FinnGene database (cases: 1198; controls: 338,286).

The study is exempt from further ethical review procedures because the statistical data used in it are freely accessible to the public and can be downloaded.

Table 1 Features of the GEO datasets utilized in the research

ID	GSE series	Disease	Control samples	Treat samples	Platform	Group
1	GSE5900	MM	22	56	GPL570	Train cohort
2	GSE6477	MM	15	147	GPL96	Train cohort
3	GSE61635	SLE	30	99	GPL570	Train cohort
4	GSE50772	SLE	20	61	GPL570	Train cohort
5	GSE118985	MM	68	682	GPL570	Test cohort
6	GSE24080	MM	0	554	GPL570	Survival cohort
7	GSE57317	MM	0	55	GPL570	Survival cohort

MM multiple myeloma, *SLE* systemic lupus erythematosus

2.2 Finding the key genes and differentially expressed genes (DEGs)

We screened the MM and SLE datasets for differentially expressed genes (DEGs) using thresholds of |logFC|> 0.585 and $p < 0.05$. The top 50 DEGs were shown as a heatmap. The intersection of upregulated and downregulated genes in the two DEG groups was then determined using a Venn diagram.

In order to investigate the relationships between the intersecting DEGs, we also created a protein–protein interaction (PPI) network for the common DEGs using STRING. We removed isolated nodes from the network and only included interaction proteins with a confidence value of ≥ 0.4. The cytoHubba plugin in Cytoscape (version 3.8.2) was used to identify key genes based on Degree and MCC values greater than 3.

2.3 Analysis of enrichment of intersecting DEGs in SLE and MM

We used R programming (version 4.4.1) to do GO and KEGG pathway enrichment analyses on the intersecting upregulated and downregulated DEGs in order to identify the pathways involved and the biological significance of these DEGs. We applied a significance threshold of $p < 0.05$.

2.4 Machine learning algorithms

We followed the methods of Bohong Chen and colleagues,by combining the two training datasets for MM (GSE5900 and GSE6477), we investigated 113 combinations of 12 machine learning algorithms, such as Lasso, Stepglm, Ridge, and Elastic Net (Enet), in accordance with the techniques of Bohong Chen and colleagues. Model construction and variable selection were done using a tenfold cross-validation framework. The performance of the model was then assessed using the validation dataset, GSE118985, as an external test dataset.

2.5 Identification of candidate drugs for drug-gene interactions

To discover candidate medications that may target the pathogenic pathways of MM and SLE, thereby building a foundation for targeted therapeutic interventions, we applied DGIdb (https://dgidb.org/) to predict potential drug interactions with the identified important genes.

2.6 MR analysis

The study includes: (1) Instrumental Variable (IV) Configuration: Using a threshold of $p < 5 \times 10\text{^}{-8}$ to identify exposures (gene eQTL data) with strong relationships. (2) Independence Assumption: The IV is independent of any unmeasured confounding factors linked to MM. (3) Exclusion Assumption: The IV is connected with MM only through eQTL and has no other relationships. During this process, we constructed cis-regulatory areas within a 10,000 kb range on either side of the coding sequences and utilized $R^2 < 0.001$ for linkage disequilibrium clustering to ensure SNP independence and reduce pleiotropic bias. Furthermore, we examined the robustness of the instrumental factors using the F-statistic ($F = \beta^2/SE^2$), with variables having $F < 10$ considered insufficient to attenuate confounding effects.

MR Egger, inverse variance weighting (IVW), weighted mode, simple mode and weighted median were the five approaches we used to analyze the data using the"TwoSampleMR"package in R software. The IVW approach served as the foundation for causal inference, and $p < 0.05$ was considered statistically significant. Additionally, we further screened data by assessing the consistency of odds ratios (OR) direction among the five approaches and verifying that heterogeneity had $p > 0.05$ as a requirement.

2.7 Immune cell infiltration

We applied the CIBERSORT tool to calculate the infiltration levels of 22 kinds of immune cells. We created an immune cell composition matrix by combining baseline data on these immune infiltrating cells. We next investigated the relationship between significant genes and immune cell infiltration, as well as the regulatory mechanisms affecting immune cells.

2.8 Identification and survival analysis of specific gene

We intersected the key genes with the results from the IVW analysis, selecting those with consistent directions of differential expression and OR as particular genes. A gene set enrichment analysis (GSEA) was done on the individual genes to evaluate the activity levels of their linked pathways, with $p < 0.05$ being statistically significant. We created a PPI network for the specified genes and assessed the results of their immune infiltration.

Additionally, we performed survival analysis on specific genes using the combined data from the GSE24080 and GSE57317 datasets. In this study, the"surv_cutpoint"function from the"survminer"package in R was used to determine the optimal cutoff value of specific genes for MM prognostic risk. Based on this cutoff, patients were categorized into low-risk and high-risk groups, and the survival curves of the two groups were compared. Furthermore, samples were grouped according to the median expression of specific genes, and differential analysis was conducted with $|logFC| > 1$ and $P < 0.05$ as the criteria. Heatmaps of the differentially expressed genes were generated, and the interactions among these genes were visualized.

2.9 Differential analysis of the MM validation groups

In order to determine if the significant genes showed differences between the control and experimental groups, we utilized R software to read the validation dataset GSE118985 (using data preprocessing techniques that were in line with those previously employed). We then compared and contrasted these results with our MR findings.

3 Results

3.1 Identification of differential expression in SLE and MM

We integrated the two training sets for MM and the two training sets for SLE described in Table 1 for later differential analysis. Next, as shown in Fig. 1A–D, we used principal component analysis (PCA) to analyze the data quality before and after batch removal, compensating for batch effects.

In the SLE cohort, a total of 1,761 DEGs were discovered, including 1,044 upregulated DEGs and 717 downregulated DEGs. The MM cohort revealed 1,213 DEGs, comprising 534 upregulated and 679 downregulated DEGs. The intersection of the DEGs from SLE and MM resulted in 63 shared genes for further investigation, with 31 being upregulated and 32 downregulate. Additionally, we visualized the top 50 DEGs from both the MM and SLE cohorts, as shown in Fig. 1.

3.2 Functional enrichment of pathogenic genes in the intersection of SLE and MM

GO enrichment analysis of the upregulated common genes revealed 605 core targets. In biological processes (BP), these targets were primarily involved in ameboidal-type cell migration (GO:0001667) and cell growth (GO:0016049). In cellular components (CC), key associations included clathrin-coated vesicles (GO:0030136) and coated vesicle membranes (GO:0030662). In molecular functions (MF), significant activities included protein heterodimerization (GO:0046982) and G protein-coupled receptor binding (GO:0001664).

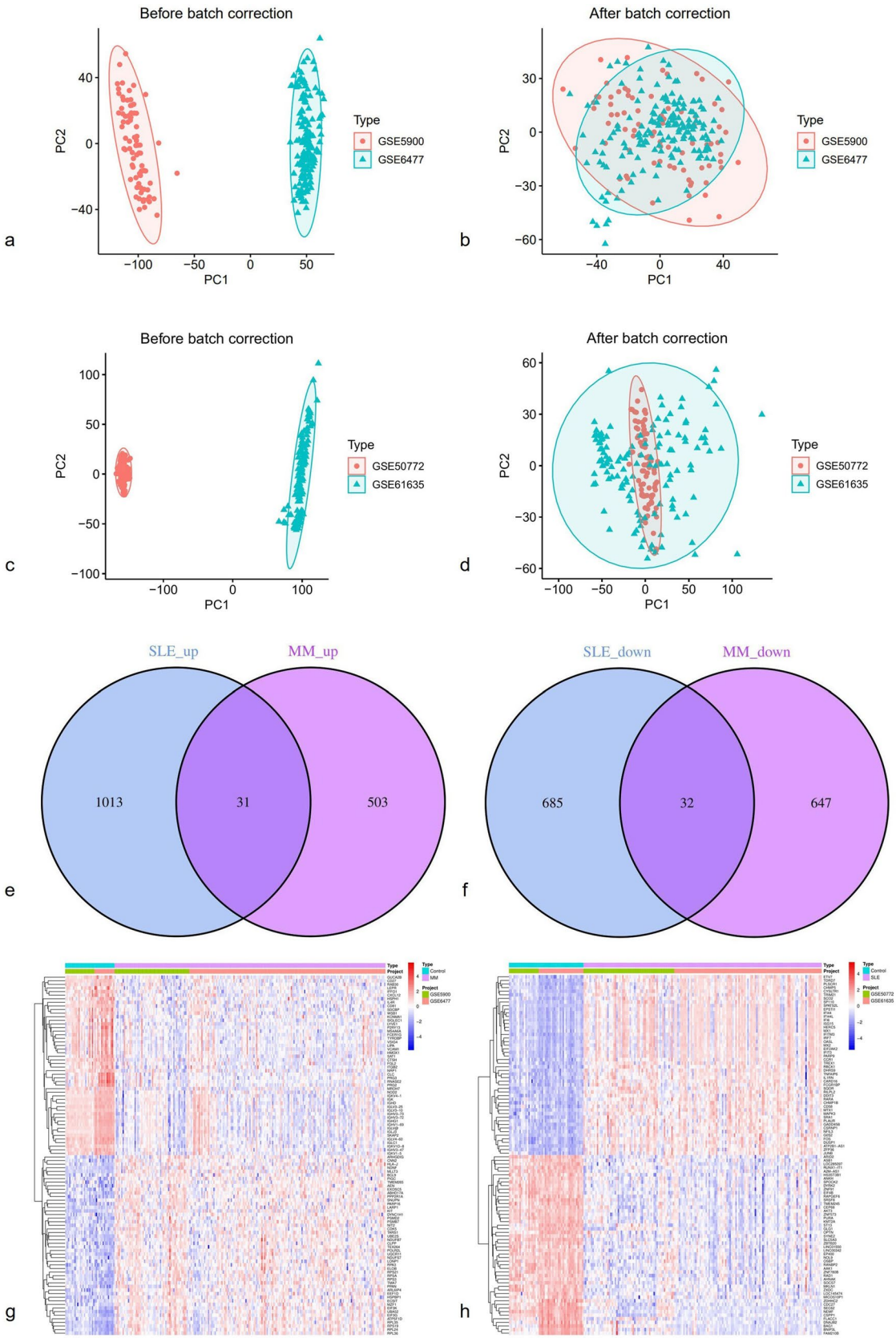

Fig. 1 **a** MM before batch adjustment. **b** MM after batch adjustment. **c** SLE before batch adjustment. **d** SLE after batch adjustment. **e** 31 upregulated common genes. **f** 32 downregulated common genes. **g** Top 50 differentially expressed genes in MM. **H** Top 50 differentially expressed genes in SLE

GO enrichment analysis of the downregulated common genes identified 292 core targets. In BP, these genes were mainly related to the immune response-activating signaling pathway (GO:0002757) and regulation of cell–cell adhesion (GO:0022407). In CC, significant terms included cell leading edge (GO:0031252) and actin-based cell projections (GO:0098858). In MF, key activities involved antigen binding (GO:0003823) and sodium ion transmembrane transporter activity (GO:0015081).

KEGG analysis of the intersecting genes indicated that the overexpressed genes primarily participate in the PI3 K-Akt signaling pathway (hsa04151), human papillomavirus infection (hsa05160), and cytokine-cytokine receptor interaction (hsa04060) (Fig. 2).

3.3 Creation of the PPI network and identification of key genes

We input the 63 common genes into STRING for interaction network analysis, removing isolated nodes, which resulted in a protein–protein interaction network comprising 38 nodes and 51 edges (Fig. 3). We then utilized the cytoHubba plugin in Cytoscape to identify key genes with both Degree and MCC values greater than 3. The identified key genes included downregulated CDH1 and IL4, and upregulated AURKB, HGF, H2BC9, H2BC17, H2BC5, and AREG, along with TJP1. We developed a visualization to help clarify the chromosomal distribution of these genes.

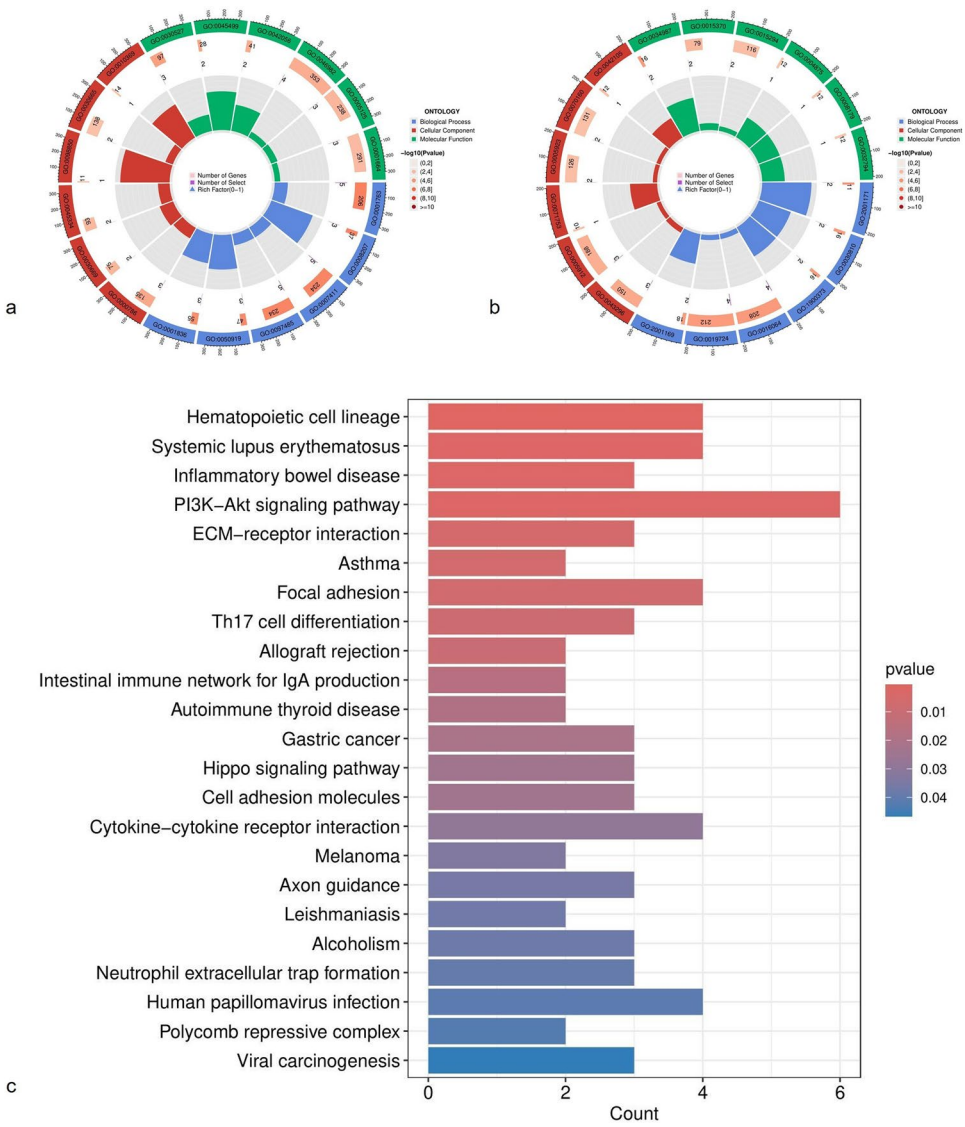

Fig. 2 **a** GO analysis of increased common genes. **b** GO analysis of downregulated common genes. **c** KEGG analysis of shared genes

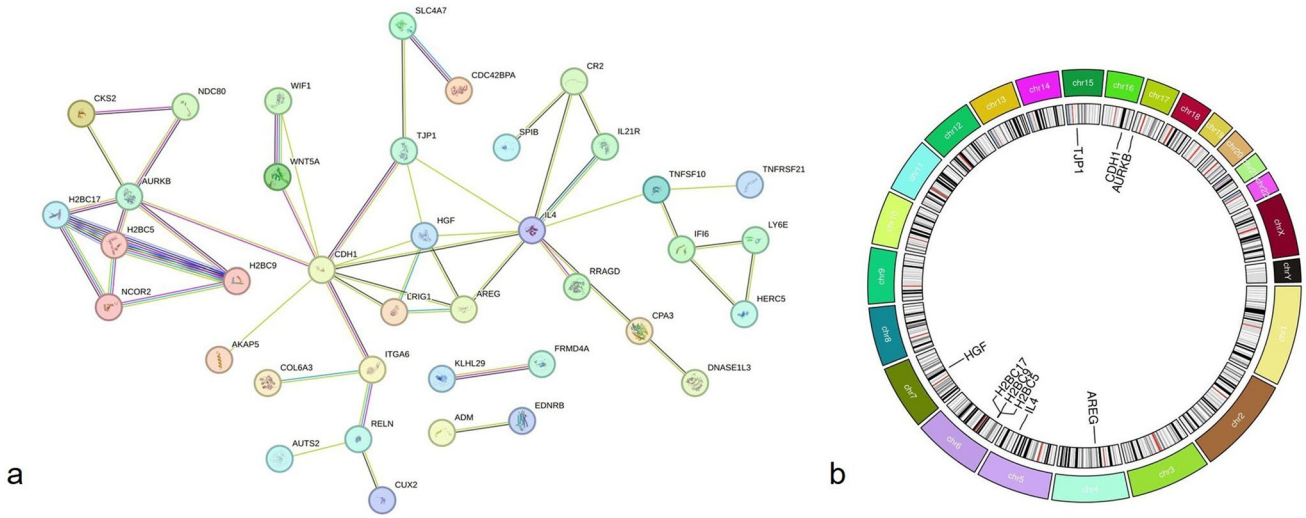

Fig. 3 **a** common genes PPI network. **b** key genes' Chromosomal distribution

3.4 Construction of the SLE-related MM diagnostic model

We utilized 113 combinations of 12 machine learning methods to construct a diagnostic model based on 9 essential genes during the tenfold cross-validation procedure. In accordance with previously published research, we determined the ideal model to be the one with the highest average AUC throughout the training and testing groups [17], ultimately developing the final model using the integrated NaiveBayes algorithm (Fig. 4).

The NaiveBayes algorithm identified all 9 key genes. As shown in Fig. 4B, the AUC values for both the training and validation sets of our diagnostic model exceeded 0.7, indicating significant accuracy and stability. Subsequent comparative analysis of the 9 key genes also revealed high AUC values: H2BC5 (AUC = 0.699), TJP1 (AUC = 0.773), CDH1 (AUC = 0.692), AURKB (AUC = 0.706), HGF (AUC = 0.762), H2BC9 (AUC = 0.780), AREG (AUC = 0.689), CR2 (AUC = 0.729), IL4 (AUC = 0.769), and H2BC17 (AUC = 0.663), demonstrating the model's robust predictive capability. Additionally, we created a nomogram including the important genes to predict MM risk, and the calibration curve further revealed a significant agreement between the observed results and anticipated risk probabilities.

3.5 Drug-gene interactions

To identify potential targeted therapies, we utilized the DGIdb database and screened a total of 33 validated drugs based on the 9 key genes. The top 10 ranked drugs based on their interactions are listed in Table 2.

3.6 Analysis of immune cell infiltration in SLE and MM

Functional and pathway investigations of the intersecting DEGs between MM and SLE indicated strong connections with immunological and inflammatory processes. Figure 5 displays the proportions of 22 immune cell types in MM and SLE samples. In the MM cohort, we detected substantial variations in the proportions of Macrophages M1, resting Mast cells, and activated Mast cells between MM and control samples. Additionally, in the SLE cohort, there was a difference in the fraction of native CD4 T cells, which was likewise lowered compared to the control group.

3.7 MR analysis

After filtering, we ultimately identified 24,389 SNPs that met the three fundamental assumptions as instrumental variables, all with F-statistics greater than 10. Through MR analysis and the defined filtering criteria, we discovered a total

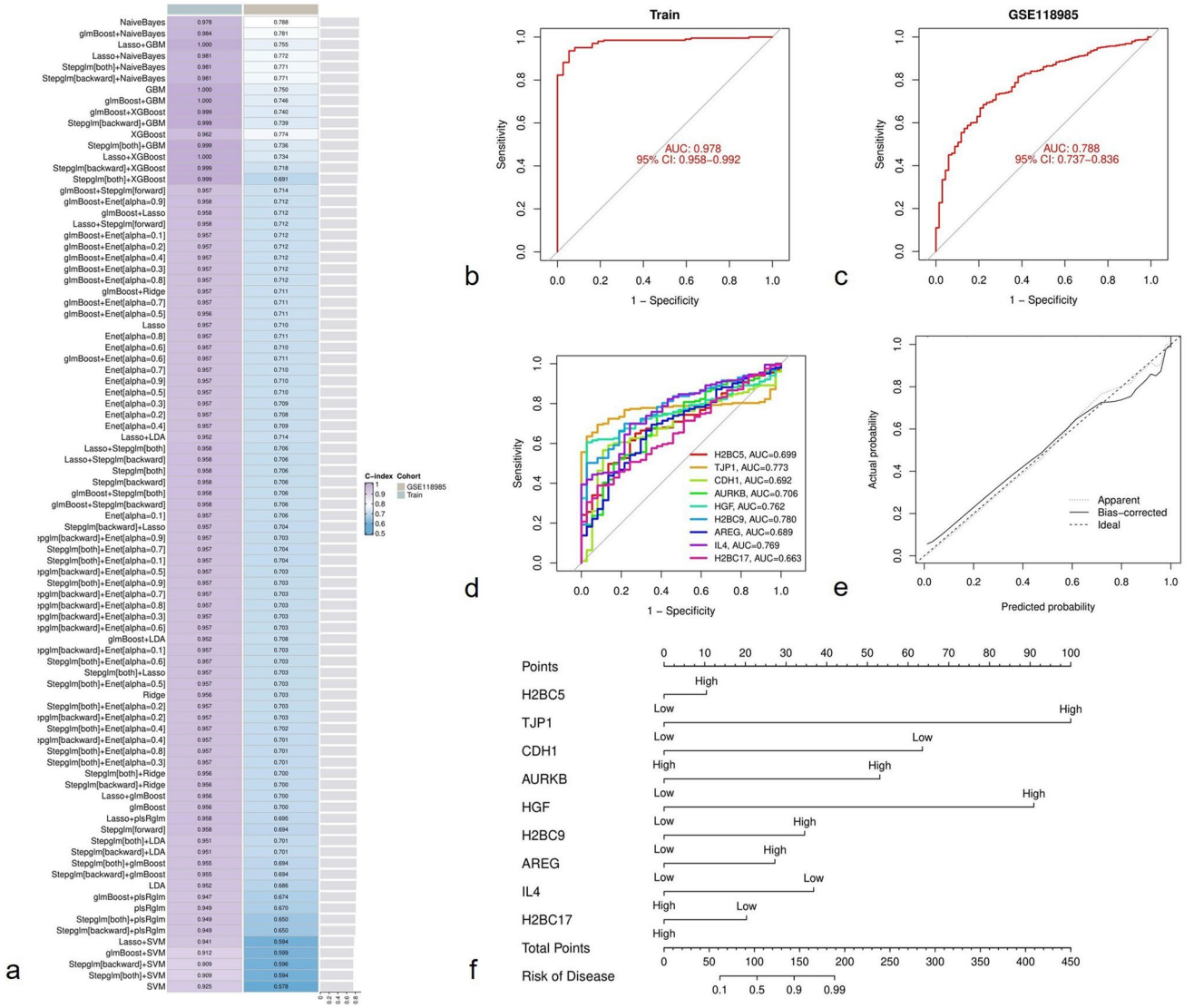

Fig. 4 **a** Assessment of the diagnostic model for SLE-related MM constructed from 113 machine learning algorithms. **b** ROC curve for the combined MM training sets (GSE5900, GSE6477). **c** ROC curve for the MM validation set. **d** ROC curves for the 9 key genes. **e** Calibration curve for the 9 key genes. **f** Nomogram incorporating the 9 key genes

Table 2 Top 10 drugs ranked by drug-gene interactions

Gene	Name	Drug	Regulatory approval	Interaction score
HGF	Hepatocyte growth factor	Gonadotropin, chorionic	Approved	1.944728564
CDH1	Cadherin 1	Bicalutamide	Approved	1.312691781
AREG	Amphiregulin	Panitumumab	Approved	0.525076712
TJP1	Tight junction protein 1	Genistein	Approved	0.452652338
AREG	Amphiregulin	Crizotinib	Approved	0.403905163
TJP1	Tight junction protein 1	Risperidone	Approved	0.391848293
AREG	Amphiregulin	Capecitabine	Approved	0.388945713
AREG	Amphiregulin	Irinotecan hydrochloride	Approved	0.33338204
TJP1	Tight junction protein 1	Dehydrated alcohol	Approved	0.332327033
TJP1	Tight junction protein 1	Dexamethasone	Approved	0.305277158

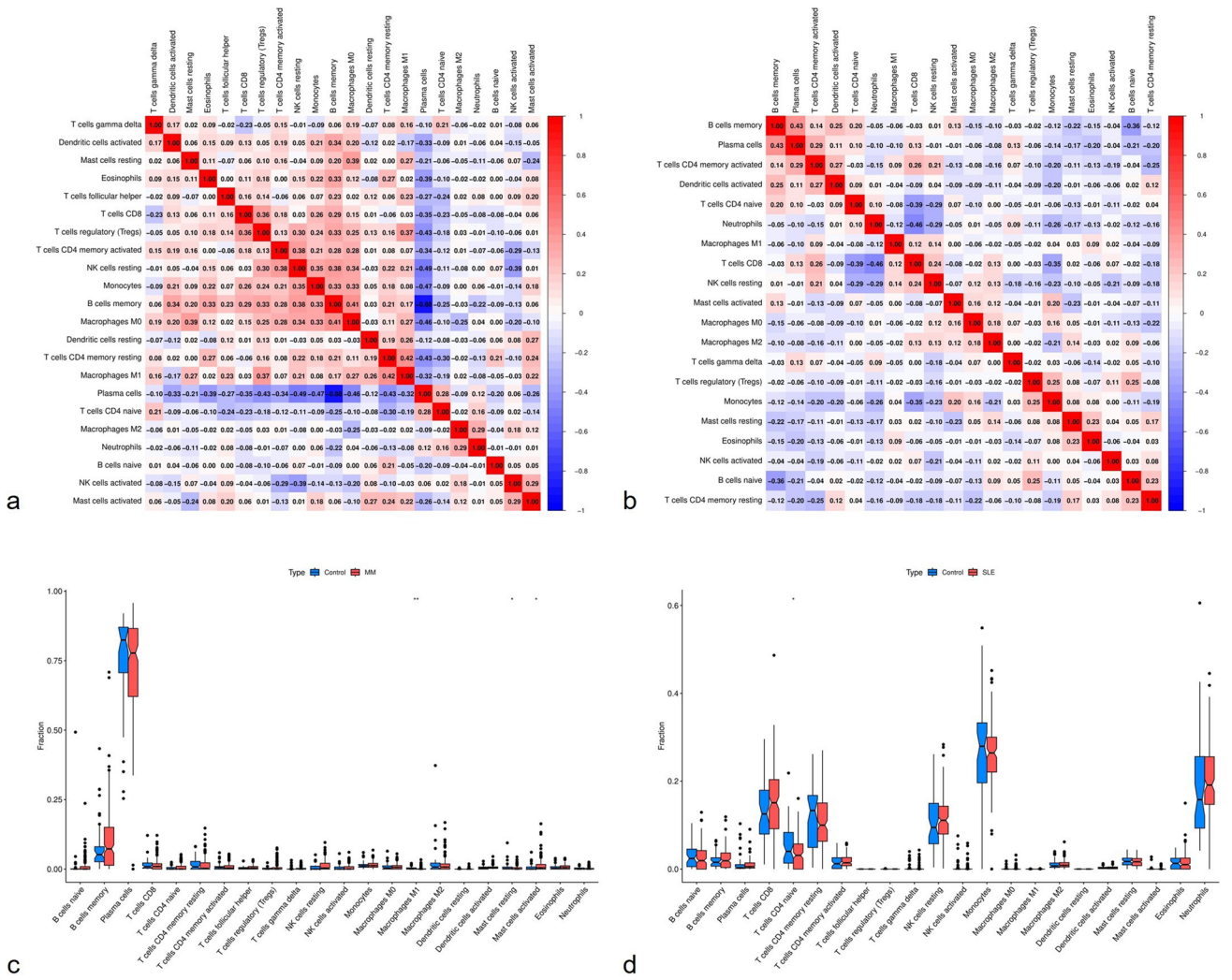

Fig. 5 **a** Immune correlation heatmap between the control and MM groups. **b** Immune correlation heatmap between the control and SLE groups. **c** 22 immune cell types are compared between the MM and control groups. **d** 22 immune cell types are compared between the SLE and control groups. (While **P < 0.01 and ***P < 0.001, *P < 0.05)

of 83 genes linked with MM. We then intersected these 83 genes with the key genes, ensuring that the direction of differential expression aligned with the OR direction. Subsequently, we conducted MR analysis on the disease-associated genes obtained from the intersection and the DEGs to explore the causal relationship of these genes with the disease.

We determined that H2BC5 may be a particular gene connected to SLE-associated MM. Using the IVW technique, we identified a substantial relationship between H2BC5 and MM risk, showing that H2BC5 increases the risk of developing MM. Figure 6 provide comprehensive details on H2BC5, including forest plots, scatter plots, leave-one-out sensitivity analysis, and funnel plots.

3.8 Identification and survival analysis of specific gene

The above study identified H2BC5 as the most relevant gene associated with SLE-related MM. We did GSEA enrichment analysis to further study the activity levels of pathways or functions connected to H2BC5. According to the findings, the top five active pathways in the H2BC5 high-expression group were systemic lupus erythematosus, oxidative phosphorylation, proteasome, ribosome, and one carbon pool via folate. On the other hand, leishmania infection, chemokine signaling, asthma, calcium signaling, and cytokine receptor interaction were the top five active pathways in the low-expression group.

a

exposure	nsnp	method	pval	OR(95% CI)
H2BC5	18	MR Egger	0.151	1.136 (0.963 to 1.341)
	18	Weighted median	0.191	1.111 (0.949 to 1.301)
	18	Inverse variance weighted	**0.033**	1.134 (1.010 to 1.273)
	18	Simple mode	0.896	1.016 (0.802 to 1.288)
	18	Weighted mode	0.110	1.128 (0.981 to 1.298)

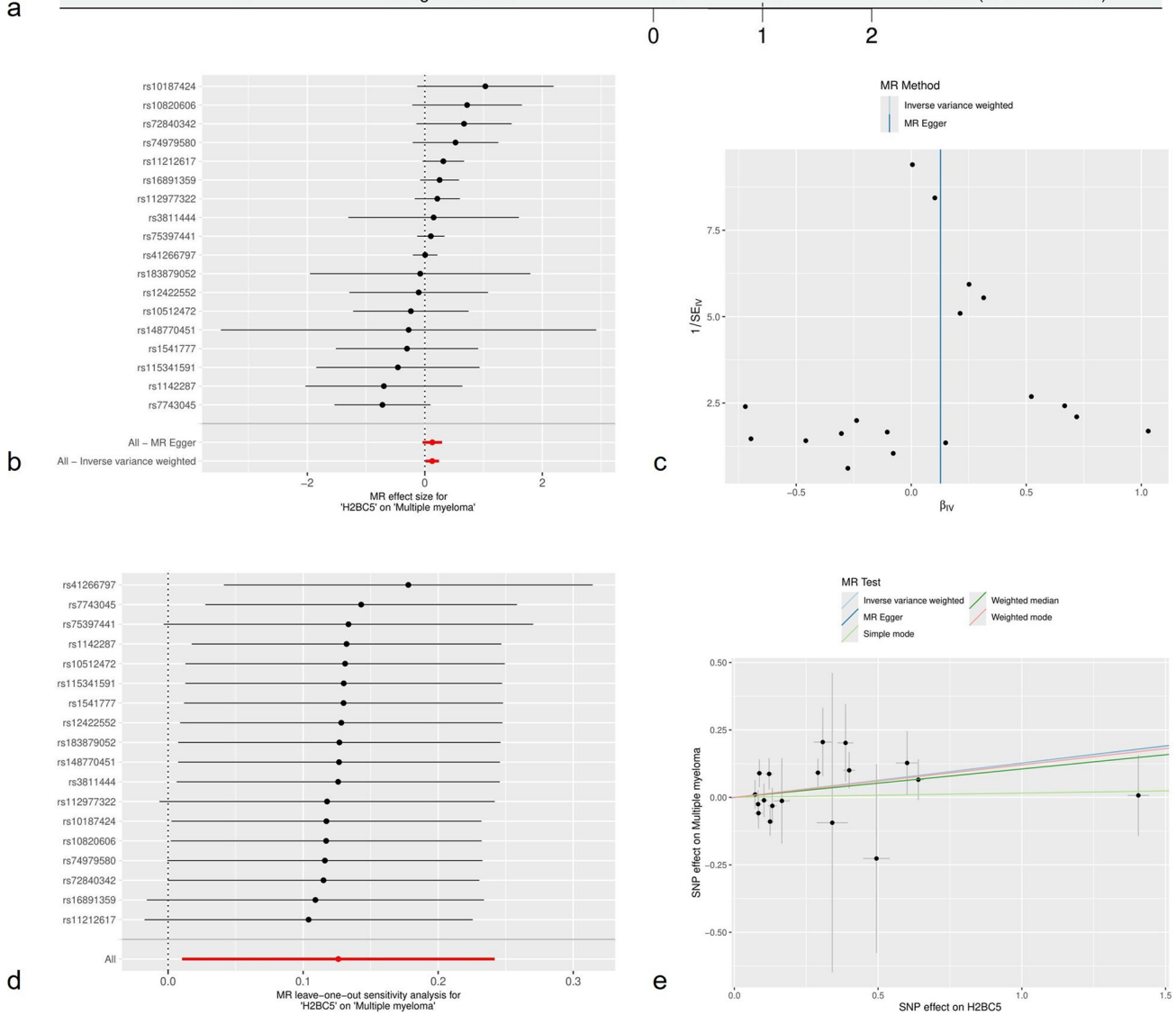

Fig. 6 **a** Forest plot illustrating the causal relationship between H2BC5 and multiple myeloma. **b** Forest plot for the MR of H2BC5. **c** Scatter plot for the MR of H2BC5. **d** Leave-one-out sensitivity analysis for the MR of H2BC5. **e** Funnel plot for the MR of H2BC5

We created a PPI network for H2BC5 using the GeneMANIA database. The results suggested that H2BC5 is predominantly engaged in tasks such as nucleosome organization, chromatin assembly, chromatin assembly or disassembly, DNA packing, protein-DNA complex subunit organization, DNA conformation change, and protein-DNA complex assembly.

Additionally, we analyzed the immune cell infiltration results of the nine key genes in the MM group. The correlation analysis of H2BC5 with 22 immune cell subtypes revealed significant associations with T cells CD4 memory resting, Macrophages M1, Plasma cells, and Neutrophils (Fig. 7).

We using the "surv_cutpoint" function, the optimal cutoff value for H2BC5 (HIST1H2BD) in MM prognostic risk was determined to be 11.88. Based on this value, MM patients were divided into a high-risk cohort (291 individuals) and a low-risk ccohort (318 individuals). The results revealed that high H2BC5 expression was significantly associated with

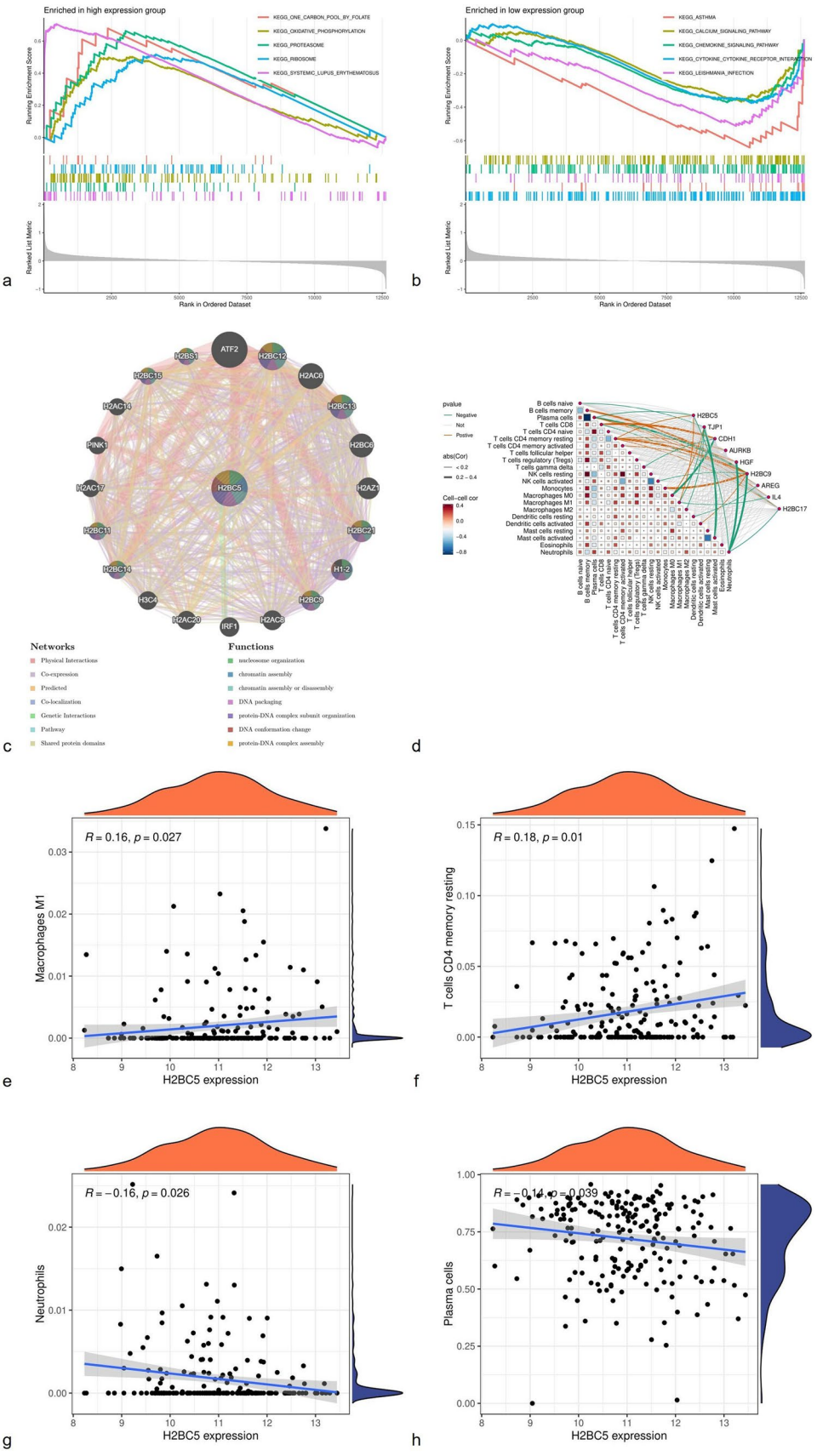

Fig. 7 **a** Top five active pathways in the high-expression group of H2BC5. **b** Top five active pathways in the low-expression group of H2BC5. **c** PPI network of H2BC5. **d** Heatmap illustrating the relationship between the nine important genes in MM and 22 immune cell types. **e** Positive correlation between H2BC5 and Macrophages M1. **f** Positive correlation between H2BC5 and T cells CD4 memory resting. **g** Negative correlation between H2BC5 and Neutrophils. **h** Negative correlation between H2BC5 and Plasma cells

poorer overall survival in multiple myeloma patients ($P < 0.05$). Furthermore, grouping based on the median expression of H2BC5 and conducting differential analysis revealed that H2BC5 expression was strongly positively correlated with H2BC6, H2BC7, H2BC9, and H2BC10, while showing a negative correlation with ADAM28 expression (Fig. 8)

3.9 Training and validation group differential analysis

The results suggest that in the validation cohort, IL4 and H2BC17 did not show significant variations between the control and validation groups, while all other important genes displayed significant variance (Fig. 9). Notably, the expression of H2BC5 in MM samples was substantially higher than that in the healthy control group, suggesting a clear difference. This elevated expression level of H2BC5, as an upregulated gene, aligns with our findings from the MR analysis, thereby enhancing the credibility of the MR results.

4 Discussion

One of the most prevalent hematological cancers, MM is frequently linked to high immunoglobulin levels. Cytokines produced by plasma cells significantly contribute to localized tissue damage, thereby creating a microenvironment conducive to the proliferation of malignant cells [20]. The pathogenesis of MM is associated with various factors, including genetic abnormalities, cytokine production, aberrant signaling pathways, and an inhibitory bone marrow microenvironment (BMM) [21–25]. Although numerous studies have reported an association between SLE and MM, the interplay between these two diseases and the underlying pathogenic mechanisms require further investigation.

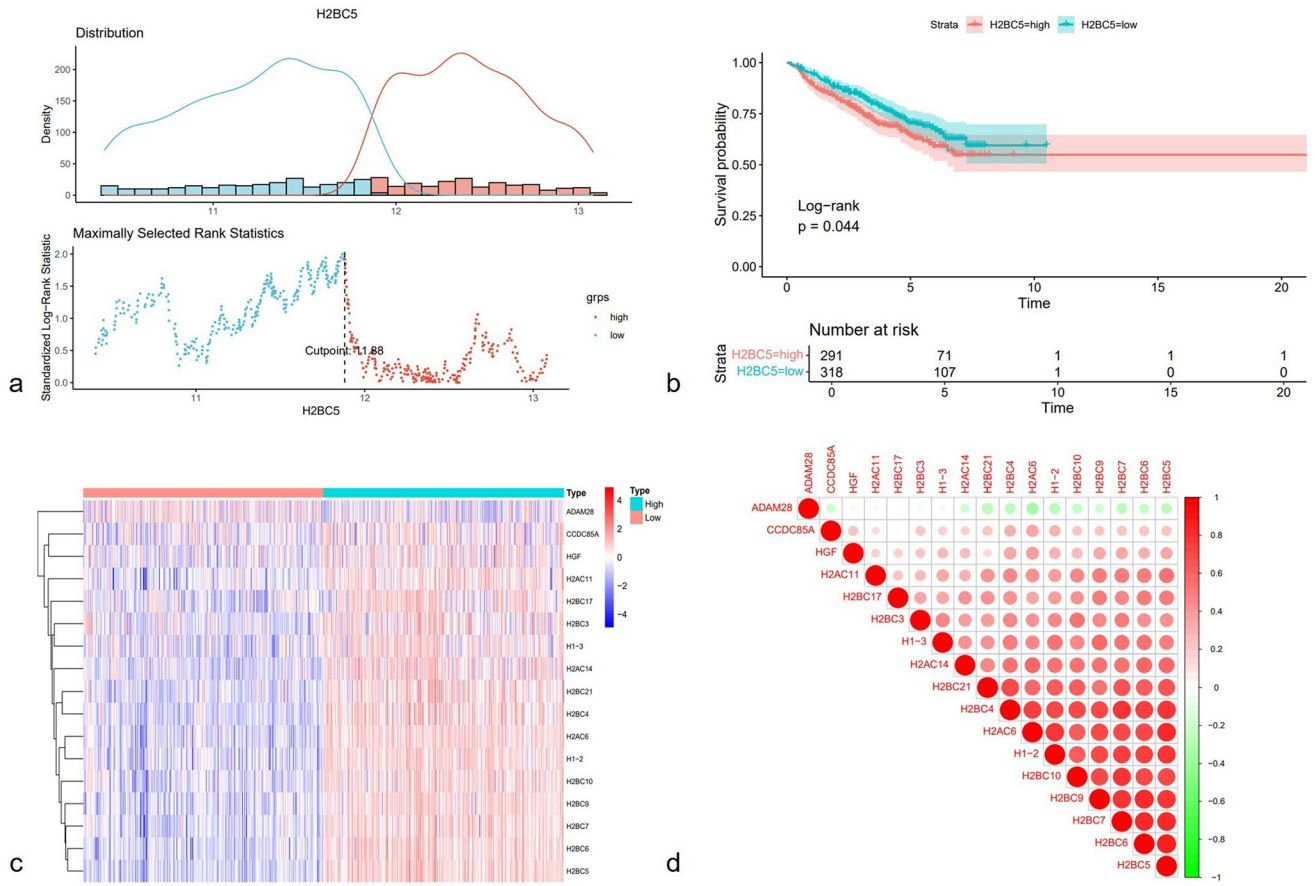

Fig. 8 **a** The optimal cutoff value of H2BC5 for predicting MM prognostic risk and the division of high and low-risk groups. Blue represents the low-risk group, and red represents the high-risk group. **b** Kaplan–Meier curve of overall survival in MM patients stratified by high and low expression of H2BC5. **c** Heatmap of differentially expressed genes identified based on the median H2BC5 expression. **d** Interaction network between H2BC5 and the identified differentially expressed genes

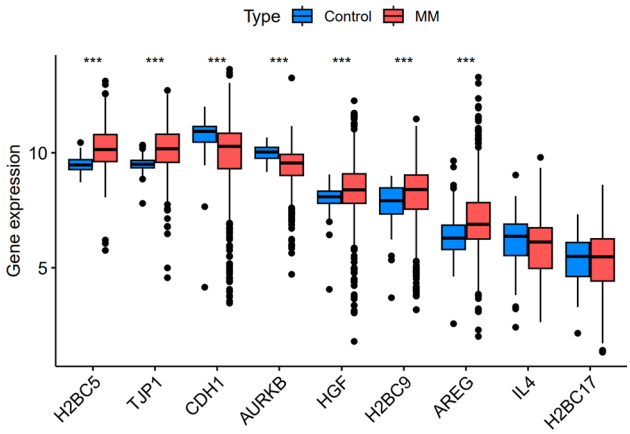

Fig. 9 Differential analysis in the MM validation group. (*P < 0.05; **P < 0.01; ***P < 0.001)

In contrast to existing studies, we employed a comprehensive approach utilizing bioinformatics and machine learning analysis to identify pathogenic genes associated with MM and constructed a diagnostic model for SLE-related MM to enhance the sensitivity of identifying potential MM in SLE patients, thereby facilitating early screening and intervention in clinical settings. We intersected the 1,213 DEGs from the MM cohort with the 1,761 DEGs from the SLE cohort, resulting in a total of 63 intersecting genes, of which 31 were upregulated and 32 were downregulated. To elucidate the underlying biological processes and pathway mechanisms linking SLE and MM, we conducted GO and KEGG enrichment analyses. In terms of GO enrichment analysis, the 31 upregulated intersecting genes primarily participate in ameboidal-type cell migration, clathrin-coated vesicle formation, and protein heterodimerization activity, while the 32 downregulated intersecting genes are predominantly involved in immune response-activating signaling pathways, cell leading edge processes, and antigen binding. Significant enrichment of overexpressed genes was found in the KEGG pathway analysis in pathways associated with human papillomavirus infection, cytokine-cytokine receptor interactions, and the PI3 K-Akt signaling pathway.

It has been shown that miR-29b inhibits the PI3 K/Akt signaling pathway and slows the proliferation of MM cells by downregulating the expression of PI3 K subunits [26]. MiR-21 overexpression in MM cells can increase cell survival and resistance to treatment by focusing on PTEN and triggering the PI3 K/Akt signaling pathway [27, 28]. The active PI3 K/Akt signaling system can enhance tumor cell motility, proliferation, and resistance through its downstream effectors, making it a potential target for anticancer therapy. Moreover, targeting and inhibiting this route has been demonstrated to improve bone deterioration in individuals with MM [29, 30]. Research has indicated that B lymphocytes play a significant role in the development of SLE. Glycolysis and oxidative phosphorylation, along with enhanced PI3 K-Akt-mTORC signaling, increase lipid synthesis, which in turn promotes B cell growth and proliferation [31–33]. The aforementioned results demonstrate that the PI3 K-Akt signaling pathway plays a key role in both SLE and MM. Furthermore, MM cells can stimulate the expression of miR-146a in mesenchymal stromal cells (MSCs), resulting in enhanced cytokine secretion, which subsequently increases the development and migration of MM cells [34].

Research reveals that inflammation plays a critical role in the relapse and medication resistance of MM [35, 36]. Iinflammatory reactions may push tumor cells to suppress the expression of antigenic proteins, hence decreasing the subsequent presentation of these antigens to the host's immune cells [37]. Inflammatory immune cells are not only engaged in the establishment of the tumor microenvironment (TME) but also contribute to tumor survival and immune regulation [38, 39]. I In the MM cohort, we observed significant differences in the proportions of M1 macrophages, resting mast cells, and activated mast cells. Research has established that the BMM plays a crucial role in the course of MM by giving survival signals and secreting growth factors that further encourage tumor proliferation. This highlights the necessity of immune treatment in MM, notably the essential role played by macrophages [40]. Furthermore, mast cells (MCs), as components of the host response, concentrate in the BMM and may contribute to the osteolytic process throughout the course of MM [41]. Similarly, SLE, being an autoimmune illness, also involves major immunological and inflammatory responses in its etiology. Compared to the control group, the fraction of natural CD4 T cells in the SLE cohort was observed to be decreased. Research reveals that autoimmune processes can lead to an increase in memory T cells and a reduction in naïve CD4 T cells [42].

We constructed the PPI network of the intersecting genes using STRING and identified 9 key genes with Degree and MCC values greater than 3 through the cytoHubba plugin in Cytoscape. Drawing on the work of Bohong Chen and

colleagues, we employed 12 different machine learning algorithms across 113 combinations to determine NaiveBayes as the optimal diagnostic model for analyzing the 9 key genes. Notably, the NaiveBayes algorithm successfully identified all 9 key genes, 7 of which have been previously demonstrated to be associated with MM.

In primordial cells from high-risk MM patients, lower levels of CDH1 are detected, which in turn encourages the proliferation of MM cells [43]. Many investigations have proven CDH1's diagnostic value as a tumor suppressor gene in MM [44, 45]. IL-4 is an efficient anti-inflammatory cytokine that can be released by numerous types of immune cells [46]. Due to its anti-angiogenic and immunosuppressive qualities, IL-4 may encourage tumor development by generating a permissive immunological environment [47, 48]. It has been established that IL-4 inhibits cell growth in a number of cancers, including lung, colorectal, renal, and breast cancers. Several studies indicate that it could be used as a biomarker for diagnosis and prognosis [49, 50]. Side population (SP) cells are a rich source of cancer stem cells with stem-like features and have been detected in several malignancies, including MM [51–54]. AURKB is significantly expressed in SP cells from both myeloma cell lines and primary MM samples [55]. The development of monoclonal gammopathy of unknown significance (MGUS) into MM depends critically on HGF [56]. Furthermore, higher expression of H2BC9 (HIST1H2BH) is related with lower survival rates in MM patients [57]. AREG, bundled within exosomes produced from MM, may represent a unique component to MM-induced osteoclastogenesis [58]. The TJP1 gene plays a vital function in cell adhesion in MM cells through epithelial-mesenchymal transition (EMT) [59].

Based on the 9 key genes, we identified a total of 33 validated drugs. The top ten drugs ranked by interaction scores are: Gonadotropin, chorionic; Bicalutamide; Panitumumab; Genistein; Crizotinib; Risperidone; Capecitabine; Irinotecan hydrochloride; Dehydrated alcohol; and Dexamethasone. These drugs may provide valuable insights for the future development of therapeutic agents for MM.

Through MR analysis and differential analysis in the validation group, we identified H2BC5 as a specific gene for diagnosing SLE-related MM. The H2B family, also known as the H2B histone family, is linked to a poor prognosis and is implicated in a number of cancer pathological processes. Histone cluster 1 H2B family member D (HIST1H2BD), also known as H2BC5, exhibits a strong positive correlation with a number of immunological indicators. Existing studies have shown that elevated expression of HIST1H2BH (H2BC9) is associated with poorer survival in MM patients and can serve as an independent prognostic factor for MM [57]. Our study found that high expression of H2BC5 adversely affects the overall survival of multiple myeloma patients and that H2BC5 expression is positively correlated with H2BC9. Furthermore, literature supports the significant role of H2BC5 in cancer. Research indicates that H2BC5 is highly expressed in glioma patients, significantly correlating with poor prognosis and serving as a high-risk factor for gliomas [60]. Interestingly, however, high expression of H2BC5 has been identified as an independent prognostic factor for better survival in cervical cancer patients, as well as being linked to SLE [61]. Additionally, the transcriptional products of H2BC5 have been confirmed as potential prognostic markers for lung cancer [62], and have been found to be upregulated in prostate cancer [63]. Based on these findings and the existing literature, we hypothesize that H2BC5 may serve as an independent prognostic factor for MM. However, since no direct studies on the effect of H2BC5 in MM have been identified, the specific impact of its high expression on MM requires further experimental validation and support.

GSEA enrichment analysis suggests that the high expression group of H2BC5 largely participates in pathways such as one carbon pool via folate, oxidative phosphorylation, proteasome, ribosome, and systemic lupus erythematosus. Studies have indicated that MM plasma cells exhibit enhanced glycolysis and oxidative phosphorylation (OXPHOS), which are traits associated with recurring genetic changes that drive MM cell proliferation and survival [64]. Research has demonstrated that proteasome inhibitors, such as bortezomib and carfilzomib, serve as foundational therapy for relapsed or refractory MM and can trigger apoptosis in malignant cells [65]. Additionally, H2BC5 is involved in functions related to nucleosome organization, chromatin assembly, and chromatin disassembly. Immune infiltration analysis demonstrates a positive correlation between H2BC5 and resting CD4 memory T cells and M1 macrophages, while revealing a negative correlation with activated plasma cells and neutrophils. As a crucial component of the bone marrow microenvironment, macrophages can inhibit proteasome pathways and block drug-induced apoptosis by interacting with signaling pathways activated by tumor cells [66].

Our research findings indicate that H2BC5 is positively correlated with T cells CD4 memory resting and Macrophages M1, while it is negatively correlated with the activation of Plasma cells and Neutrophils, suggesting a potential close relationship between H2BC5 and the immune microenvironment. Previous studies have found that H2BC5 is associated with autoimmune diseases, including SLE and rheumatoid arthritis [67]. Moreover, elevated levels of myeloma-associated macrophages have been linked to poor prognosis in MM [68], whereas neutrophils play a significant role in inhibiting tumor growth and metastasis [69]. The number of granulocytes in the bone marrow can serve as an additional parameter for assessing MM progression. A higher proportion of neutrophils in newly

diagnosed MM patients is often associated with improved overall survival, and their reduction can predict adverse outcomes in MM [70]. Additionally, the proliferation, progression, and survival of malignant plasma cells (PC) in MM are highly regulated by the bone marrow microenvironment [71]. Mesenchymal stem cells (MSCs) are known to induce an immunosuppressive microenvironment that may facilitate the progression from MGUS to MM [38]. Notably, during human MSC differentiation, the fraction of polyadenylated H2BC5 transcripts increases [72]. Unfortunately, we have not yet found relevant literature on the role of H2BC5 in the tumor microenvironment.

H2BC5 is directly associated with the risk of MM, and its diagnostic value has been elucidated and validated in the aforementioned studies. However, no research has yet addressed the direct relationship between H2BC5 and MM In future studies, we plan to further investigate and experimentally validate the function of H2BC5 in the progression of multiple myeloma and its immune microenvironment.

5 Summary

Overall, our findings present a novel molecular framework for the early detection of MM, particularly in individuals with SLE. The aim is to research the shared pathogenic pathways between SLE and MM and to develop treatment strategies linking the two illnesses. This study focuses on nine genes: CDH1, IL4, AURKB, HGF, H2BC9, H2BC17, H2BC5, AREG, and TJP1. Interestingly, seven of these genes have been linked to MM in the past. Furthermore, our study highlights the diagnostic value of H2BC5 in relation to SLE-associated MM risk, indicating its direct correlation with MM risk and presenting a promising avenue for further research.

6 Limitations

Due to constraints in experimental conditions, this study primarily relies on bioinformatics approaches and machine learning algorithms, lacking validation through clinical patients, animal models, or cell-level experiments, which inevitably limits the reliability of the findings. Additionally, H2BC5 has been identified as a gene specifically associated with SLE-related MM, underscoring its potential as a biomarker. However, its role in the diagnosis and identification of MM warrants further investigation.

Author contributions Yuepei Liu: Manuscript writing, formal analysis, data organization, conceptualization, visualization. Songshan Liu: Review and editing, conceptualization, methodology.

Funding This study did not receive any financing from public, commercial, or non-profit entities.

Data availability Data is provided within the manuscript or supplementary information files.

Declarations

Ethics approval and consent to participate This study adheres to local legislation and institutional requirements, and does not require approval from an institutional review board.

Competing interests The authors declare no competing interests.

References

1. Luo H, Pan C, Wang L, Zheng L, Cao S, Hu X, Hu T, Zhao N, Shang Q, Wang J. Low TYROBP expression predicts poor prognosis in multiple myeloma. Cancer Cell Int. 2024;24(1):117.
2. Li J, Dong J, Li M, Zhu H, Xin P. Potential mechanisms for predicting comorbidity between multiple myeloma and femoral head necrosis based on multiple bioinformatics. Comput Biol Chem. 2024;113: 108220.
3. Bumma N, Dhakal B, Fraser R, Estrada-Merly N, Anderson K, Freytes CO, Hildebrandt GC, Holmberg L, Krem MM, Lee C, et al. Impact of bortezomib-based versus lenalidomide maintenance therapy on outcomes of patients with high-risk multiple myeloma. Cancer. 2023;129(14):2179–91.
4. Huang J, Chan SC, Lok V, Zhang L, Lucero-Prisno DE 3rd, Xu W, Zheng ZJ, Elcarte E, Withers M, Wong MCS. The epidemiological landscape of multiple myeloma: a global cancer registry estimate of disease burden, risk factors, and temporal trends. Lancet Haematol. 2022;9(9):e670–7.
5. Mateos MV, San Miguel JF. Management of multiple myeloma in the newly diagnosed patient. Hematology Am Soc Hematol Educ Program. 2017;2017(1):498–507.
6. Shah N, Chari A, Scott E, Mezzi K, Usmani SZ. B-cell maturation antigen (BCMA) in multiple myeloma: rationale for targeting and current therapeutic approaches. Leukemia. 2020;34(4):985–1005.
7. Ren J, Wu M. Causal effects of genetically determined blood metabolites on multiple myeloma: a Mendelian randomization study. Sci Rep. 2023;13(1):18818.
8. Su X, Yu H, Lei Q, Chen X, Tong Y, Zhang Z, Yang W, Guo Y, Lin L. Systemic lupus erythematosus: pathogenesis and targeted therapy. Molecular biomedicine. 2024;5(1):54.
9. Choi MY, Flood K, Bernatsky S, Ramsey-Goldman R, Clarke AE. A review on SLE and malignancy. Best Pract Res Clin Rheumatol. 2017;31(3):373–96.
10. Han JY, Kim H, Jung SY, Jang EJ, Cho SK, Sung YK. Increased risk of malignancy in patients with systemic lupus erythematosus: population-based cohort study in Korea. Arthritis Res Ther. 2021;23(1):270.
11. Desai R, Devaragudi S, Kaur L, Singh K, Bawa J, Theik NWY, Palisetti S, Jain A. SLE and multiple myeloma: an underlooked link? A review of case reports from the last decade. J Med Life. 2024;17(2):141–6.
12. Lian L, Wang K, Xu S. Systemic lupus erythematosus associated with multiple myeloma: Two case reports and a literature review. Immun Inflamm Dis. 2023;11(1): e755.
13. Basha FKM, Reddy VT, Sharma P, Vaishnav B. An interesting case of systemic lupus erythematosus with multiple myeloma. J Fam Med Prim Care. 2023;12(11):2970–2.
14. Kiriakidou M, Ching CL. Systemic lupus erythematosus. Ann Int Med. 2020. https://doi.org/10.7326/AITC202006020.
15. Chen PH, Tung HH, Lin CH, Huang KP, Ni YL, Lin CY. A case report of secondary synchronous diagnosis of multiple myeloma and systemic lupus erythematosus after breast cancer treatment: a CARE-compliant article. Medicine. 2022;101(35): e30320.
16. Eyuboglu S, Alpsoy S, Uversky VN, Coskuner-Weber O. Key genes and pathways in the molecular landscape of pancreatic ductal adenocarcinoma: a bioinformatics and machine learning study. Comput Biol Chem. 2024;113: 108268.
17. Chen B, Sun X, Huang H, Feng C, Chen W, Wu D. An integrated machine learning framework for developing and validating a diagnostic model of major depressive disorder based on interstitial cystitis-related genes. J Affect Disord. 2024;359:22–32.
18. Davies NM, Holmes MV, Davey Smith G. Reading Mendelian randomisation studies: a guide, glossary, and checklist for clinicians. BMJ Clin Res. 2018;362: k601.
19. Hu R, Chen F, Yu X, Li Z, Li Y, Feng S, Liu J, Li H, Shen C, Gu X, et al. Construction and validation of a prognostic model of angiogenesis-related genes in multiple myeloma. BMC Cancer. 2024;24(1):1269.
20. Lu W, Huang H, Xu Z, Xu S, Zhao K, Xiao M. MiR-27a inhibits the growth and metastasis of multiple myeloma through regulating Th17/Treg balance. PLoS ONE. 2024;19(10): e0311419.
21. Neuse CJ, Lomas OC, Schliemann C, Shen YJ, Manier S, Bustoros M, Ghobrial IM. Genome instability in multiple myeloma. Leukemia. 2020;34(11):2887–97.
22. Gu C, Wang W, Tang X, Xu T, Zhang Y, Guo M, Wei R, Wang Y, Jurczyszyn A, Janz S, et al. CHEK1 and circCHEK1_246aa evoke chromosomal instability and induce bone lesion formation in multiple myeloma. Mol Cancer. 2021;20(1):84.
23. Akhtar S, Ali TA, Faiyaz A, Khan OS, Raza SS, Kulinski M, Omri HE, Bhat AA, Uddin S. Cytokine-mediated dysregulation of signaling pathways in the pathogenesis of multiple myeloma. Int J Mol Sci. 2020. https://doi.org/10.3390/ijms21145002.
24. Gau YC, Yeh TJ, Hsu CM, Hsiao SY, Hsiao HH. Pathogenesis and treatment of myeloma-related bone disease. Int J Mol Sci. 2022. https://doi.org/10.3390/ijms23063112.
25. Lu Q, Yang D, Li H, Niu T, Tong A. Multiple myeloma: signaling pathways and targeted therapy. Mol Biomed. 2024;5(1):25.
26. Yan B, Guo Q, Fu FJ, Wang Z, Yin Z, Wei YB, Yang JR. The role of miR-29b in cancer: regulation, function, and signaling. Onco Targets Ther. 2015;8:539–48.
27. Handa H, Murakami Y, Ishihara R, Kimura-Masuda K, Masuda Y. The role and function of microrna in the pathogenesis of multiple myeloma. Cancers. 2019. https://doi.org/10.3390/cancers11111738.
28. Alimohammadi M, Rahimzadeh P, Khorrami R, Bonyadi M, Daneshi S, Nabavi N, Raesi R, Farani MR, Dehkhoda F, Taheriazam A, et al. A comprehensive review of the PTEN/PI3K/Akt axis in multiple myeloma: From molecular interactions to potential therapeutic targets. Pathol Res Pract. 2024;260: 155401.
29. Gan ZY, Fitter S, Vandyke K, To LB, Zannettino AC, Martin SK. The effect of the dual PI3K and mTOR inhibitor BEZ235 on tumour growth and osteolytic bone disease in multiple myeloma. Eur J Haematol. 2015;94(4):343–54.
30. Lu W, Liu J, Luo M, Xiao M. Relationship between monoclonal gammopathy of undetermined significance and multiple myeloma via online database analysis. Pak J Med Sci. 2023;39(3):715–20.
31. Jacobi AM, Mei H, Hoyer BF, Mumtaz IM, Thiele K, Radbruch A, Burmester GR, Hiepe F, Dörner T. HLA-DRhigh/CD27high plasmablasts indicate active disease in patients with systemic lupus erythematosus. Ann Rheum Dis. 2010;69(1):305–8.

32. Caro-Maldonado A, Wang R, Nichols AG, Kuraoka M, Milasta S, Sun LD, Gavin AL, Abel ED, Kelsoe G, Green DR, et al. Metabolic reprogramming is required for antibody production that is suppressed in anergic but exaggerated in chronically BAFF-exposed B cells. J Immunol. 2014;192(8):3626–36.
33. Iwata S, Hajime Sumikawa M, Tanaka Y. B cell activation via immunometabolism in systemic lupus erythematosus. Front Immunol. 2023;14:1155421.
34. De Veirman K, Wang J, Xu S, Leleu X, Himpe E, Maes K, De Bruyne E, Van Valckenborgh E, Vanderkerken K, Menu E, et al. Induction of miR-146a by multiple myeloma cells in mesenchymal stromal cells stimulates their pro-tumoral activity. Cancer Lett. 2016;377(1):17–24.
35. Greten FR, Grivennikov SI. Inflammation and cancer: triggers, mechanisms, and consequences. Immunity. 2019;51(1):27–41.
36. Zhao Q, Li F, Li J, Xia Y, Wang J, Chen L. An inflammatory response-related gene signature can predict the prognosis and impact the immune infiltration of multiple myeloma. Clin Exp Med. 2024;24(1):16.
37. Ricketts TD, Prieto-Dominguez N, Gowda PS, Ubil E. Mechanisms of macrophage plasticity in the tumor environment: manipulating activation state to improve outcomes. Front Immunol. 2021;12: 642285.
38. de Jong MME, Kellermayer Z, Papazian N, Tahri S, Hofste Op Bruinink D, Hoogenboezem R, Sanders MA, van de Woestijne PC, Bos PK, Khandanpour C, et al. The multiple myeloma microenvironment is defined by an inflammatory stromal cell landscape. Nat Immunol. 2021;22(6):769–80.
39. Kawano Y, Roccaro AM, Ghobrial IM, Azzi J. Multiple Myeloma and the Immune Microenvironment. Curr Cancer Drug Targets. 2017;17(9):806–18.
40. Zheng Y, Yang J, Qian J, Qiu P, Hanabuchi S, Lu Y, Wang Z, Liu Z, Li H, He J, et al. PSGL-1/selectin and ICAM-1/CD18 interactions are involved in macrophage-induced drug resistance in myeloma. Leukemia. 2013;27(3):702–10.
41. Vyzoukaki R, Tsirakis G, Pappa CA, Devetzoglou M, Tzardi M, Alexandrakis MG. The impact of mast cell density on the progression of bone disease in multiple myeloma patients. Int Arch Allergy Immunol. 2015;168(4):263–8.
42. Ugarte-Gil MF, Sánchez-Zúñiga C, Gamboa-Cárdenas RV, Aliaga-Zamudio M, Zevallos F, Tineo-Pozo G, Cucho-Venegas JM, Mosqueira-Riveros A, Perich-Campos RA, Alfaro-Lozano JL, et al. Circulating naive and memory CD4+ T cells and metabolic syndrome in patients with systemic lupus erythematosus: data from a primarily Mestizo population. Rheumatology (Oxford). 2015;54(7):1302–7.
43. Lub S, Maes A, Maes K, De Veirman K, Leleu X, Menu E, De Bruyne E, Vanderkerken K, Van Valckenborgh EJB. Targeting the anaphase promoting complex/Cyclosome (APC/C) in multiple myeloma. Blood. 2014;124(21):2097.
44. Peng Y, Wu D, Li F, Zhang P, Feng Y, He A. Identification of key biomarkers associated with cell adhesion in multiple myeloma by integrated bioinformatics analysis. Cancer Cell Int. 2020;20:262.
45. Paiva B, Martinez-Lopez J, Corchete LA, Sanchez-Vega B, Rapado I, Puig N, Barrio S, Sanchez ML, Alignani D, Lasa M, et al. Phenotypic, transcriptomic, and genomic features of clonal plasma cells in light-chain amyloidosis. Blood. 2016;127(24):3035–9.
46. Serin I, Oyaci Y, Pehlivan M, Pehlivan S. Role of cytokines in multiple myeloma: IL-1RN and IL-4 VNTR polymorphisms. Cytokine. 2022;153: 155851.
47. Ma J, Liu D, Mao X, Huang L, Ren Y, Xu X, Huang X, Deng C, Shi F, Sun P. Enhanced diagnostic efficiency of endometrial carcinogenesis and progression in women with abnormal uterine bleeding through peripheral blood cytokine testing: a multicenter retrospective cohort study. Int J Med Sci. 2024;21(4):601–11.
48. Wang HW, Joyce JA. Alternative activation of tumor-associated macrophages by IL-4: priming for protumoral functions. Cell cycle (Georgetown, Tex). 2010;9(24):4824–35.
49. Fu C, Jiang L, Hao S, Liu Z, Ding S, Zhang W, Yang X, Li S. Activation of the IL-4/STAT6 signaling pathway promotes lung cancer progression by increasing M2 myeloid cells. Front Immunol. 2019;10:2638.
50. Kozłowski M, Borzyszkowska D, Lerch N, Turoń-Skrzypińska A, Tkacz M, Lubikowski J, Tarnowski M, Rotter I, Cymbaluk-Płoska A. IL-4, IL-7, IL-9, NT, NRP1 may be useful markers in the diagnosis of endometrial cancer. Biomolecules. 2024. https://doi.org/10.3390/biom14091095.
51. Challen GA, Little MH. A side order of stem cells: the SP phenotype. Stem cells (Dayton, Ohio). 2006;24(1):3–12.
52. Jakubikova J, Adamia S, Kost-Alimova M, Klippel S, Cervi D, Daley JF, Cholujova D, Kong SY, Leiba M, Blotta S, et al. Lenalidomide targets clonogenic side population in multiple myeloma: pathophysiologic and clinical implications. Blood. 2011;117(17):4409–19.
53. Patrawala L, Calhoun T, Schneider-Broussard R, Zhou J, Claypool K, Tang DG. Side population is enriched in tumorigenic, stem-like cancer cells, whereas ABCG2+ and ABCG2- cancer cells are similarly tumorigenic. Can Res. 2005;65(14):6207–19.
54. Chiba T, Miyagi S, Saraya A, Aoki R, Seki A, Morita Y, Yonemitsu Y, Yokosuka O, Taniguchi H, Nakauchi H, et al. The polycomb gene product BMI1 contributes to the maintenance of tumor-initiating side population cells in hepatocellular carcinoma. Can Res. 2008;68(19):7742–9.
55. Nara M, Teshima K, Watanabe A, Ito M, Iwamoto K, Kitabayashi A, Kume M, Hatano Y, Takahashi N, Iida S, et al. Bortezomib reduces the tumorigenicity of multiple myeloma via downregulation of upregulated targets in clonogenic side population cells. PLoS ONE. 2013;8(3): e56954.
56. Hofmann JN, Landgren O, Landy R, Kemp TJ, Santo L, McShane CM, Shearer JJ, Lan Q, Rothman N, Pinto LA, et al. A prospective study of circulating chemokines and angiogenesis markers and risk of multiple myeloma and its precursor. JNCI Cancer Spectr. 2020. https://doi.org/10.1093/jncics/pkz104.
57. Zhang W, Chen X, Wang Z, Wang Q, Feng J, Wang D, Wang Z, Tang J, Qing S, Zhang Y. Identification of HIST1H2BH as the hub gene associated with multiple myeloma using integrated bioinformatics analysis. Hematology. 2024;29(1):2335421.
58. Raimondo S, Saieva L, Vicario E, Pucci M, Toscani D, Manno M, Raccosta S, Giuliani N, Alessandro R. Multiple myeloma-derived exosomes are enriched of amphiregulin (AREG) and activate the epidermal growth factor pathway in the bone microenvironment leading to osteoclastogenesis. J Hematol Oncol. 2019;12(1):2.
59. Li M, Qi L, Xu JB, Zhong LY, Chan S, Chen SN, Shao XR, Zheng LY, Dong ZX, Fang TL, et al. Methylation of the promoter region of the tight junction protein-1 by DNMT1 induces EMT-like features in multiple myeloma. Mol Ther Oncol. 2020;19:197–207.
60. Jia J, Han Z, Wang X, Zheng X, Wang S, Cui Y. H2B gene family: a prognostic biomarker and correlates with immune infiltration in glioma. Front Oncol. 2022;12: 966817.
61. Li X, Tian R, Gao H, Yang Y, Williams BRG, Gantier MP, McMillan NAJ, Xu D, Hu Y, Gao Y. Identification of a histone family gene signature for predicting the prognosis of cervical cancer patients. Sci Rep. 2017;7(1):16495.

62. Zeng Z, Lu J, Wu D, Zuo R, Li Y, Huang H, Yuan J, Hu Z. Poly(ADP-ribose) glycohydrolase silencing-mediated H2B expression inhibits benzo(a) pyrene-induced carcinogenesis. Environ Toxicol. 2021;36(3):291–7.
63. Lin HP, Jiang SS, Chuu CP. Caffeic acid phenethyl ester causes p21 induction, Akt signaling reduction, and growth inhibition in PC-3 human prostate cancer cells. PLoS ONE. 2012;7(2): e31286.
64. Bloedjes TA, de Wilde G, Khan GH, Ashby TC, Shaughnessy JD, Zhan F, Houtkooper RH, Bende RJ, van Noesel CJM, Spaargaren M, et al. AKT supports the metabolic fitness of multiple myeloma cells by restricting FOXO activity. Blood Adv. 2023;7(9):1697–712.
65. Wesley CD, Sansonetti A, Neutel CHG, Krüger DN, De Meyer GRY, Martinet W, Guns PJ. Short-term proteasome inhibition: assessment of the effects of carfilzomib and bortezomib on cardiac function, arterial stiffness, and vascular reactivity. Biology. 2024;13(10):2.
66. De Beule N, De Veirman K, Maes K, De Bruyne E, Menu E, Breckpot K, De Raeve H, Van Rampelbergh R, Van Ginderachter JA, Schots R, et al. Tumour-associated macrophage-mediated survival of myeloma cells through STAT3 activation. J Pathol. 2017;241(4):534–46.
67. Ramezankhani R, Minaei N, Haddadi M, Solhi R, Taleahmad S. The impact of sex on susceptibility to systemic lupus erythematosus and rheumatoid arthritis; a bioinformatics point of view. Cell Signal. 2021;88: 110171.
68. Komohara Y, Jinushi M, Takeya M. Clinical significance of macrophage heterogeneity in human malignant tumors. Cancer Sci. 2014;105(1):1–8.
69. Xie C, Zhong L, Luo J, Luo J, Wu Y, Zheng S, Jiang L, Zhang J, Shi Y. Identification of mutation gene prognostic biomarker in multiple myeloma through gene panel exome sequencing and transcriptome analysis in Chinese population. Comput Biol Med. 2023;163: 107224.
70. Cheng Y, Sun F, Alapat DV, Wanchai V, Mery D, Siegel ER, Xu H, Johnson S, Guo W, Bailey C, et al. Multi-omics reveal immune microenvironment alterations in multiple myeloma and its precursor stages. Blood Cancer J. 2024;14(1):194.
71. Giannakoulas N, Ntanasis-Stathopoulos I, Terpos E. The role of marrow microenvironment in the growth and development of malignant plasma cells in multiple myeloma. Int J Mol Sci. 2021. https://doi.org/10.3390/ijms22094462.
72. Kari V, Karpiuk O, Tieg B, Kriegs M, Dikomey E, Krebber H, Begus-Nahrmann Y, Johnsen SA. A subset of histone H2B genes produces polyadenylated mRNAs under a variety of cellular conditions. PLoS ONE. 2013;8(5): e63745.